IEEE Access
Multidisciplinary | Rapid Review | Open Access Journal

Received October 19, 2019, accepted November 7, 2019, date of publication November 12, 2019,
date of current version November 25, 2019.

Digital Object Identifier 10.1109/ACCESS.2019.2953073

A Robust High-Order Disturbance Observer Design for SDRE-Based Suboptimal Speed Controller of Interior PMSM Drives

MUHAMMAD SAAD RAFAQ, ANH TUAN NGUYEN, HAN HO CHOI, (Member, IEEE), AND JIN-WOO JUNG, (Member, IEEE)
Division of Electronics and Electrical Engineering, Dongguk University, Seoul 04620, South Korea

Corresponding author: Jin-Woo Jung (jinwjung@dongguk.edu)

This work was supported by the Basic Science Research Program under the National Research Foundation of Korea (NRF) through the Ministry of Education under Grant 2018R1D1A1B07046873.

ABSTRACT This paper proposes a robust high-order disturbance observer (HODO) for the state-dependent Riccati equation (SDRE)-based suboptimal speed controller of an interior permanent magnet synchronous motor (IPMSM) drive. The conventional disturbance observers (DOs) cannot accurately estimate the fast time-varying disturbances of an IPMSM during the transient-state because the disturbances are assumed to change slowly, so the inaccurately estimated disturbances lead to conservative robust control. Unlike the conventional DOs, the proposed HODO guarantees the fast convergence of the estimated error for an IPMSM drive by accurately estimating the fast time-varying disturbances and their all high-order derivatives. Also, it is specifically applicable to the SDRE based suboptimal speed controller which cannot completely eliminate the steady-state error in the presence of mismatched disturbances and uncertainties. Finally, the simulation results via a MATLAB/Simulink package and the experimental results via a prototype IPMSM test-bed having TI TMS320F28335 DSP are presented to verify the faster dynamic response, smaller steady-state error, and more robust response of the SDRE speed controller with the proposed HODO compared with the conventional 1st-order DO, conventional generalized proportional integral observer (GPIO), and conventional SDRE observer.

INDEX TERMS High-order disturbance observer (HODO), interior permanent magnet synchronous motor (IPMSM), state dependent Riccati equation (SDRE), suboptimal speed controller.

I. INTRODUCTION

For the past few decades, electric vehicles (EVs), spindle drives, robotics, and air-conditioners have encouraged the researchers to work on interior permanent magnet synchronous motor (IPMSM) drives with attractive characteristics such as high torque density, compact size, wide speed range operation, and robust rotor structure [1]. In order to efficiently utilize the high torque-to-current ratio of an IPMSM, the control strategies based on maximum torque per ampere (MTPA) trajectory are developed by calculating the optimum references for the d-q axis currents [2]. However, the IPMSM drives always confront the disturbances which include the fast time-varying quantities associated with the fast electrical dynamics such as parameter uncertainties (e.g., variations in the stator resistance, d-q axis inductances, magnet flux linkage, etc.) and unmodeled dynamics (e.g., measurement error effects, dead-time effects, etc.) and the slow time-varying quantities associated with the mechanical dynamics (e.g., load torque, rotor inertia, viscous friction coefficient, etc.) [3], [4]. The d-q axis inductances depend on the level of magnetic saturation in the iron which is the function of the d-q axis currents (i_d and i_q), so the rate of variations in the d-q axis inductances is relatively fast compared to the mechanical parameters of the IPMSM. On the other hand, the parameters of the IPMSM relatively vary slowly due to the temperature effects [3]. These disturbances should be appropriately attenuated to accurately regulate the

The associate editor coordinating the review of this manuscript and approving it for publication was Yan-Jun Liu.

rotor speed of the IPMSMs because they can highly degrade the transient and steady-state tracking performance of the IPMSM drives [5].

The classical linear control techniques such as proportional integral (PI) controller [5] and linear quadratic regulator (LQR) [6] cannot provide the precise tracking performance and robustness during the transient and steady-state operations because the disturbances cannot be completely attenuated. Meanwhile, the state-dependent Riccati equation (SDRE) based suboptimal controller [7], which is a nonlinear version of the LQR optimal control, is applied to precisely control the speed of the IPMSM drives that are also subject to the adverse effects of the disturbances and high computational burden for gain calculation. However, the performance of the classical linear control and SDRE techniques can be greatly improved by incorporating the disturbance attenuation methods [8].

In recent years, disturbance observers (DOs) are commonly utilized to estimate the disturbances (e.g., load torque, motor parameters uncertainties, unmodeled dynamics etc.) of the IPMSMs and these estimated disturbances are used in the feedforward control to attenuate the disturbances [9]. For an IPMSM drive, the DOs can be classified into three types according to what is estimated as follows: DOs to estimate the load torque [10]–[14], DOs to estimate the parameter uncertainties and unmodeled dynamics [15]–[19], and DOs to estimate both the load torque, parameter uncertainties, and unmodeled dynamics [20]–[22]. First, the DOs for load torque estimation are designed to precisely estimate the unknown load torque in real-time while the other mechanical uncertainties associated with the load torque are completely ignored [10]. In [11], the performance of the nonlinear optimal load torque observer is dependent on the motor parameters and the extensive tuning efforts of the weighting matrices are required to achieve the fast convergence. In [12], the moving horizon estimator (MHE) is designed to estimate the load torque of the induction motors but it introduces noise and overshoot tendency to the speed control loop. An active flux-based observer using the principle of the MHE is also reported for the IPMSM but the tradeoff between the horizon length and the computation cost needs further research to improve the overall control performance [13]. With these techniques mentioned above [10]–[14], sensorless torque control can be efficiently implemented but the unattended disturbances are still in the system, which deteriorate the control performance. Second, the DOs for parameter uncertainties estimation are designed to identify the variations in motor mechanical parameters while ignoring the variations in the electrical parameters of the PMSM [15]. In [16], only motor parameters are estimated by using a sliding mode observer (SMO) to compensate for the disturbances associated with parameter variations, but the chattering phenomenon degrades its performance. A least square approach based on the black-box is used to compensate for the unmodeled dynamics of the IPMSM [17]. However, the results of the estimated parameters are not clearly reported to highlight the impact of the estimated parameters. The extended Kalman filter (EKF) is used for the online parameter identification of the PMSM and it is reported that the complexity of the EKF is much higher than other methods [18]. In [19], the model reference adaptive system (MRAS) method for parameter estimation is simple and easy to implement, but it is sensitive to adaptation gains. Thus, in cases of the DOs for the load torque [10]–[14] and the parameter uncertainties [15]–[19], the overall control performance of the drive systems may deteriorate due to the presence of the unattended disturbances. Last, the DO [20] is designed to estimate the offset caused by the parameter uncertainties and load torque, but it does not show any results of the estimated disturbances for a more clear analysis. Moreover, the conventional DOs have to set some bounded conditions [21] and utilize the conventional assumption that the disturbances vary slowly relative to the observer dynamics to assure its respective stability and convergence [22]. In [23]–[25], the convergence of the DOs is guaranteed by using the conventional assumption that the disturbances vary slowly relative to the observer dynamics. Therefore, during the transient-state, the disturbances associated with the fast electrical dynamics change quickly [26], so the conventional DOs do not accurately estimate the fast time-varying disturbances, which result in the conservative robustness to the speed control of an IPMSM. Meanwhile, an adaptive DO such as a generalized proportional integral observer (GPIO) [27] is used to suppress the offsets caused by the negative effects of the lumped disturbances by incorporating very high gains. Also, another adaptive DO [28] with the complex design is developed to reject the disturbances of the PMSM. Hence, the IPMSMs require a DO that can precisely estimate the fast-time varying disturbances during the transient and steady-state operations in order to achieve the robust speed control. Additionally, unlike an SPMSM drive, the DOs on the IPMSM require more research efforts due to its complexity and susceptibility to the disturbances in the presence of the magnetic saliency [29]. However, a few researches have been found on the high-order DOs to accurately estimate the disturbances for the aerodynamic applications [30]. Meanwhile, a nonsmooth extension of the GPIO is investigated to estimate the high-order disturbances only for the general class of nonlinear systems [31].

In order to accurately estimate the fast time-varying disturbances, this paper presents a high-order disturbance observer (HODO) design that can be utilized in most speed control techniques of an IPMSM drive for the disturbance compensation. The main contributions of the proposed HODO compared to the conventional DOs are summarized as: (*i*) Relaxation of the conventional assumption via *Assumption 1* to quickly estimate the fast time-varying disturbances and their high-order disturbances; (*ii*) Utilization of the high-order integral terms to precisely estimate the fast time-varying disturbances during the transient and steady-state; (*iii*) Calculation of the optimum order for the proposed HODO (see Section IV-B). Also, the disturbances estimated by the proposed HODO can be used to various applications

such as controller design, condition monitoring, fault analysis, etc. In order to highlight the faster dynamic response, smaller steady-state error (SSE), and more robust response of the proposed technique, the comparative experimental performance evaluation of the state-dependent Riccati equation (SDRE) speed controller [7] with the proposed HODO, the conventional the 1st-order DO [20], the conventional GPIO [27], and the conventional SDRE observer [7] is carried out through a MATLAB/Simulink package and a prototype IPMSM testbed with TI TMS320F28335 DSP.

II. DYNAMIC MODEL OF AN IPMSM WITH UNCERTAINTIES

In the synchronously rotating d-q reference frame, the speed and stator voltage equations are expressed as [3]

$$\begin{aligned}\dot{\omega}_r &= k_1 i_q - k_2\omega_r + k_{10} i_d i_q + \sigma_\omega \\ \dot{i}_q &= -k_3 i_q - k_4\omega_r + k_5 v_q - k_9\omega_r i_d + \sigma_q \\ \dot{i}_d &= -k_6 i_d + k_7 v_d + k_8\omega_r i_q + \sigma_d \end{aligned} \tag{1}$$

where

$$k_1 = \frac{3}{2J}\frac{p^2}{4}\lambda_m, \quad k_2 = \frac{B}{J}, \; k_3 = \frac{R_s}{L_q},$$
$$k_4 = \frac{\lambda_m}{L_q}, \quad k_5 = \frac{1}{L_q}, \; k_6 = \frac{R_s}{L_d}, \quad k_7 = \frac{1}{L_d}, \; k_8 = \frac{L_q}{L_d},$$
$$k_9 = \frac{L_d}{L_q}, \quad k_{10} = \frac{3}{2J}\frac{p^2}{4}\left(L_d - L_q\right),$$

and v_d, v_q, i_d, and i_q are the stator voltages and currents in the rotating d-q frame, ω_r is the electrical rotor angular speed, T_L is the load torque, R_s is the stator resistance, L_d and L_q are the stator d-q axis inductance in the rotating d-q reference frame, λ_m is the magnet flux linkage, J is the rotor inertia, B is the viscous friction coefficient, and p is the number of poles. Also, σ_ω, σ_q, and σ_d are the lumped disturbances associated with ω_r, i_q, and i_d, respectively, which are presented as [3], [4]

$$\begin{aligned}\sigma_\omega &= \Delta k_1 i_q - \Delta k_2\omega_r - (k_{11} + \Delta k_{11})T_L + \Delta k_{10} i_d i_q + \varepsilon_\omega \\ \sigma_q &= -\Delta k_3 i_q - \Delta k_4\omega_r - \Delta k_9\omega_r i_d + \Delta k_5 v_q + \varepsilon_q \\ \sigma_d &= -\Delta k_6 i_d + \Delta k_7 v_d + \Delta k_8\omega_r i_q + \varepsilon_d \end{aligned} \tag{2}$$

where $\Delta k_{11} = -p\Delta J/(2J(J+\Delta J))$ such that $\Delta k_{11} + k_{11} = p/(2(J+\Delta J))$ and $k_{11} = p/(2J)$; ε_ω, ε_q, and ε_d are the unstructured uncertainties due to the unmodeled dynamics; and T_L is the load torque which is generally an unknown disturbance to be rejected. $\Delta k_1, \ldots, \Delta k_{11}$ are the uncertainties of the parameters $k_1, \ldots, k_{11}$, respectively that are required to be compensated for to achieve the robust control performance.

III. HIGH-ORDER DISTURBANCE OBSERVER FOR SDRE BASED SUBOPTIMAL SPEED CONTROLLER DESIGN

First, the proposed HODO design is presented to estimate the disturbances of an IPMSM and then these estimated disturbances are utilized by the SDRE based suboptimal speed controller [7] to mitigate the disturbances. Next, the overall stability of the proposed HODO-based SDRE speed controller is verified for an IPMSM drive.

A. HIGH-ORDER DISTURBANCE OBSERVER DESIGN

This subsection designs the proposed high-order disturbance observer (HODO) which accurately estimates the lumped disturbance $\boldsymbol{\sigma} = [\sigma_\omega, \sigma_q, \sigma_d]^T$ in the dynamic model (1) of an IPMSM, which can be rewritten as the following state space model:

$$\dot{\boldsymbol{x}}_{\boldsymbol{o}} = \boldsymbol{A}_{\boldsymbol{o}}(\boldsymbol{x}_{\boldsymbol{o}})\boldsymbol{x}_{\boldsymbol{o}} + \boldsymbol{B}\boldsymbol{u}_{\boldsymbol{o}} + \boldsymbol{\sigma} \tag{3}$$

where $\boldsymbol{u}_{\boldsymbol{o}} = \begin{bmatrix} v_q & v_d \end{bmatrix}^T$, $\boldsymbol{\sigma} = \begin{bmatrix} \sigma_\omega & \sigma_q & \sigma_d \end{bmatrix}^T$,

$$\boldsymbol{A}_{\boldsymbol{o}}(\boldsymbol{x}_{\boldsymbol{o}}) = \begin{bmatrix} -k_2 & k_1 & k_{10} i_q \\ -k_4 - k_9 i_d & -k_3 & 0 \\ k_8 i_q & 0 & -k_6 \end{bmatrix},$$
$$\boldsymbol{B} = \begin{bmatrix} 0 & 0 \\ k_5 & 0 \\ 0 & k_7 \end{bmatrix}, \quad \boldsymbol{x}_{\boldsymbol{o}} = \begin{bmatrix} \omega_r \\ i_q \\ i_d \end{bmatrix}.$$

Unlike the conventional DOs, the proposed HODO utilizes the high-order integral terms in its design such that the values of the time-varying disturbance $\boldsymbol{\sigma}$ and their corresponding all high-order derivatives can be quickly and accurately estimated. The conventional assumption that the disturbance varies slowly relative to the observer dynamics, i.e., $\dot{\boldsymbol{\sigma}}(t) \approx 0$ is employed to ensure the stability of the conventional DOs, but this assumption leads to conservative robustness to the speed tracking control. In order to weaken the conventional assumption (i.e., $\dot{\boldsymbol{\sigma}}(t) \approx 0$) and design the proposed HODO that ensures the fast estimation of $\boldsymbol{\sigma}$, a relaxed assumption is used as follows.

Assumption 1: The disturbance $\boldsymbol{\sigma}(t)$ in (3) can be represented as $\boldsymbol{\sigma}(t) = \sum_{i=0}^{k} \boldsymbol{\sigma}_k t^k$ which is not necessarily constant, but it is smooth enough, i.e., there exists a large enough positive integer k such that $\boldsymbol{\sigma} \in R^k$. Moreover, it is assumed that the k-th order derivative of the disturbance is bounded, i.e., $|\boldsymbol{\sigma}^k| \leq \kappa$ and slowly time-varying during a small sampling period T_s such that $\boldsymbol{\sigma}^k d(t)/dt^k = 0$ provided that $\kappa \in R$ is a bounded constant.

It should be noted that $\boldsymbol{\sigma}$ can be expressed as a Taylor series expansion of time such that the order is infinitive. In this paper, *Assumption 1* is used to truncate the disturbance function at the kth-order, so it is reasonable and useful in practice.

The proposed kth-order HODO for estimating the $\boldsymbol{\sigma}$ in (3) is designed as

$$\begin{aligned}\dot{\boldsymbol{z}} &= \boldsymbol{A}_{\boldsymbol{o}}\boldsymbol{x}_{\boldsymbol{o}} + \boldsymbol{B}\boldsymbol{u}_{\boldsymbol{o}} + \hat{\boldsymbol{\sigma}} \\ \hat{\boldsymbol{\sigma}} &= \boldsymbol{L}_{\boldsymbol{0}}\boldsymbol{g} + \boldsymbol{L}_{\boldsymbol{1}}\boldsymbol{g}_{\boldsymbol{1}} + \cdots + \boldsymbol{L}_{\boldsymbol{k}}\boldsymbol{g}_{\boldsymbol{k}} \\ \boldsymbol{g} &= \boldsymbol{x}_{\boldsymbol{o}} - \boldsymbol{z} \\ \dot{\boldsymbol{g}}_{\boldsymbol{1}} &= \boldsymbol{g} \\ &\vdots \\ \dot{\boldsymbol{g}}_{\boldsymbol{k}} &= \boldsymbol{g}_{\boldsymbol{k-1}}. \end{aligned} \tag{4}$$

where $\boldsymbol{z}$ is the internal state variable, $\hat{\boldsymbol{\sigma}}$ is an estimate of the $\boldsymbol{\sigma}$, $\boldsymbol{g}_k$ represents the kth derivative of the argument function, and $\boldsymbol{L}_0, \boldsymbol{L}_1, \ldots, \boldsymbol{L}_k$ are the gains of the disturbance observer which can be represented as, $\boldsymbol{L}_i = diag\,\{l_{i1}, \ldots, l_{ij}\}$ such that $i = (0,$

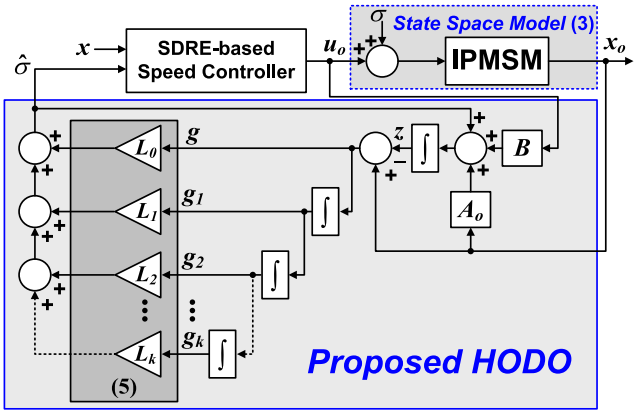

FIGURE 1. Schematic block diagram of the proposed HODO.

$1, \ldots, k$), k is the order of the HODO, $j = (1, 2, \ldots, r)$, and r is the dimension of $\boldsymbol{\sigma}$ in (3). Fig. 1 presents the schematic block diagram of the proposed HODO in which $\boldsymbol{x}$ represents the tracking error of the IPMSM.

The convergent dynamics can be assigned separately by using the r-characteristic polynomial equations for all $j = (1, 2, \ldots, r)$ and $i = (0, 1, \ldots, k)$. The observer gains $\boldsymbol{L}_i = diag\{l_{i1}, \ldots, l_{ij}\}$ are calculated corresponding to the Hurwitz polynomials:

$$\begin{aligned} p_1(s) &= s^{i+1} + l_{01}\, s^{i} + l_{11}\, s^{i-1} + \cdots + l_{i1} \\ &\vdots \\ p_j(s) &= s^{i+1} + l_{0j}\, s^{i} + l_{1j}\, s^{i-1} + \cdots + l_{ij} \end{aligned} \tag{5}$$

where (5) is Hurwitz stable. The convergent dynamics of the proposed HODO are achieved by appropriately selecting l_{ij} corresponding to the characteristic polynomials such that $p_1(s) = 0; \ldots; p_j(s) = 0$ where $j = (1, 2, \ldots, r)$. Then the estimated disturbance $\boldsymbol{\sigma}$ in (4) asymptotically converges to its real value. It is noted that the tuning mechanism can be achieved by following the conventional pole placement approach [32], and in MATLAB, the pole placement can be performed by using the commands "place" or "acker". In this paper, the popular Ackermann's formula is used for the online pole placement of the proposed HODO that also works for the time-varying poles of the IPMSM model [33].

Define the estimation error as

$$\boldsymbol{e} = \boldsymbol{\sigma} - \hat{\boldsymbol{\sigma}}. \tag{6}$$

Then from the first and third equations of (4), (6) can be rewritten as

$$\boldsymbol{e} = \dot{\boldsymbol{g}}. \tag{7}$$

Based on (7) and other equations in (4) through some manipulations, it follows that

$$\dot{\boldsymbol{e}} = \begin{bmatrix} \dot{\boldsymbol{e}}_1 \\ \dot{\boldsymbol{e}}_2 \\ \vdots \\ \dot{\boldsymbol{e}}_k \end{bmatrix} = \underbrace{\begin{bmatrix} \boldsymbol{0} & \boldsymbol{I} & \cdots & \\ \boldsymbol{0} & \boldsymbol{0} & \boldsymbol{I} & \\ \vdots & & \ddots & \\ -\boldsymbol{L_0} & -\boldsymbol{L_1} & \cdots & -\boldsymbol{L_k} \end{bmatrix}}_{\boldsymbol{L}} \boldsymbol{e}. \tag{8}$$

where $(\boldsymbol{e})_{(k)}$ and $(\cdot)^{(k)}$ denote the kth derivative of the argument function. By referring to *Assumption 1*, $\boldsymbol{\sigma}^{(k+1)} = 0$, which implies that the steady-state estimation error $\mathbf{e}$ is zero according to Hurwitz stability condition.

In *Assumption 1*, it is considered that $\boldsymbol{\sigma}^k d(t)/dt^k = 0$. This implies that the kth-order of the HODO is required to be designed. On the other hand, the unknown structure of the lumped disturbance $\boldsymbol{\sigma}(t)$ of the IPMSM makes the order determination of the HODO difficult.

Remark 1: The order of the designed HODO is determined to optimize its performance at different operating conditions. In this regard, a positive but small enough real number γ is pre-designated in case that it is difficult to obtain the analytical expression of the disturbance. If there exists a positive integer m such that $||\boldsymbol{g}_{m+1}|| < \gamma$, then $k = m$ [34].

Remark 2: The conventional GPIO [27], the conventional nonsmooth observer [31], and the proposed HODO can be used to estimate the high-order disturbances which can also be represented as the exosystems. Due to the presence of the integral terms, the proposed HODO shows a little resemblance with the conventional GPIO and the conventional nonsmooth observer, but they are generically different. As presented in (4), the presence of the internal state variable $\boldsymbol{z}$ decouples the IPMSM state $\boldsymbol{x}_o$ from the disturbance estimation error dynamics. As the proposed HODO state $\boldsymbol{z}$ does not follow the system state $\boldsymbol{x}_o$, the disturbance estimation error dynamics is completely decoupled from the system state (or the observer state). This implies that it is not required for $\hat{\boldsymbol{x}}_o$ to reach $\boldsymbol{x}_o$ within a finite time or as time goes to infinity. Thus, the estimation error dynamics becomes simple. In addition, this decoupling from the IPMSM states simplifies the stability analysis of the proposed HODO. On the other hand, the conventional GPIO employs the reference or desired state values to estimate the disturbances of the IPMSM [27] and the conventional nonsmooth observer uses the measured state values to estimate the disturbances. Thus, both the conventional GPIO and the conventional nonsmooth observer are coupled with the system states such that $\hat{\boldsymbol{x}}_o$ should approach $\boldsymbol{x}_o$ as time goes to infinity or within finite time.

Remark 3: The *Assumption 1* presenting $\boldsymbol{\sigma}^k d(t)/dt^k = \boldsymbol{\sigma}^{(k+1)} = 0$ is quite relaxed compared to the conventional assumption, i.e., $\dot{\boldsymbol{\sigma}}(t) \approx 0$ [22], [23], [35] which ignores the higher-order disturbances encountered in the IPMSM drives. Note that the estimation of the higher-order disturbances makes the proposed HODO dynamically fast compared to the conventional observers [30]. Next, the *Assumption 1* bounds the k-th order derivative of the disturbance $\boldsymbol{\sigma}^k$ such that

$\boldsymbol{\sigma}^k d(t)/dt^k = 0$, which is used to prove the stability of the proposed HODO. In addition, the *Assumption 1* states that the disturbance varies slowly during the small sampling time T_s (e.g., $T_s = 200\ \mu$s in this paper), so the sinusoidal disturbance, i.e., sin $(\omega_r t + b)$ will be smooth enough during T_s and then satisfies the *Assumption 1*. This verifies that the sinusoidal disturbances will be smooth enough during the small T_s [5]. Thus, the *Assumption 1* is quite relaxed for the sampling time T_s compared with the common conventional assumption, i.e., $\dot{\boldsymbol{\sigma}}(t) \approx 0$ [22], [23].

Remark 4: The sampling time T_s is delimited by the characteristics of the hardware setup used for the implementation [36]. The optimal fast tracking HODO bandwidth should be less than the inverse of the sampling time T_s. However, it is not appropriate to maximize the bandwidth of the proposed HODO [37]. Higher observer bandwidth maximizes the response to measurement noise. Therefore, the observer bandwidth is intentionally set to a lower value, i.e., 5 times smaller than the maximum possible bandwidth value to minimize the noise sensitivity.

B. HIGH-ORDER DISTURBANCE OBSERVER-BASED SDRE SPEED CONTROLLER DESIGN AND STABILITY ANALYSIS

This subsection describes the utilization of the estimated $\boldsymbol{\sigma}$ to the SDRE based speed controller [7] for the disturbance attenuation, and then analyzes the stability of the proposed HODO-based SDRE speed controller for an IPMSM drive. The tracking errors of the ω_r, i_q, and i_d are represented as

$$\tilde{\omega} = \omega_r - \omega_d, \quad \tilde{i}_q = i_q - i_{qd}, \ \tilde{i}_d = i_d - i_{dd} \tag{9}$$

where $\omega_d, \tilde{\omega}$ are the desired rotor speed and rotor speed error; $\tilde{i}_q$, $\tilde{i}_d$ are the current errors of the i_q, and i_d, respectively; i_{qd}, i_{dd} are the desired current references of the i_q and i_d, respectively which can be set by the following approximate equations [7]:

$$i_{qd} = \frac{k_2\omega_d + \dot{\omega}_d - k_{10} i_{dd} i_q - \sigma_\omega}{k_1 + k_{10}\tilde{i}_d} \approx \frac{k_2\omega_d - k_{10} i_{dd} i_q - \sigma_\omega}{k_1} \tag{10a}$$

$$i_{dd} = \frac{L_d - L_q}{\lambda_m} i_{qd}^2. \tag{10b}$$

It is assumed that the desired references (i.e., ω_d, i_{qd}, and i_{dd}) change very slowly during the small sampling time T_s which implies that the derivative of the desired references is zero [4]. Then the dynamic model (1) of an IPMSM can be transformed into the following error dynamics state-dependent form:

$$\dot{\boldsymbol{x}} = \boldsymbol{A}(\boldsymbol{x})\boldsymbol{x} + \boldsymbol{B}(\boldsymbol{u} + \boldsymbol{u_{com}} + \boldsymbol{\sigma_c}) \tag{11}$$

where

$$\boldsymbol{A}(\boldsymbol{x}) = \begin{bmatrix} -k_2 & k_1 & k_{10}\tilde{i}_q \\ -k_4 - k_9\tilde{i}_d & -k_3 & 0 \\ k_8\tilde{i}_q & 0 & -k_6 \end{bmatrix},$$

$$\boldsymbol{B} = \begin{bmatrix} 0 & 0 \\ k_5 & 0 \\ 0 & k_7 \end{bmatrix}, \quad \boldsymbol{x} = \begin{bmatrix} \tilde{\omega} \\ \tilde{i}_q \\ \tilde{i}_d \end{bmatrix}, \quad \boldsymbol{\sigma_c} = \begin{bmatrix} \sigma_q \\ \sigma_d \end{bmatrix},$$

$\boldsymbol{u} = [u_q, u_d]^T$ are the dq-axis stabilizing control terms, and $\boldsymbol{u}_{com}$ are the dq-axis compensating control terms designed as

$$\boldsymbol{u_{com}} = \begin{bmatrix} u_{cq} \\ u_{cd} \end{bmatrix} = \begin{bmatrix} \frac{1}{k_5}\left(k_3 i_{qd} + k_4\omega_d + k_9\tilde{i}_d\omega_d + k_9 i_{dd}\omega_r\right) \\ \frac{1}{k_7}\left(k_6 i_{dd} - k_8\tilde{i}_q\omega_d - k_8 i_{qd}\omega_r\right) \end{bmatrix}. \tag{12}$$

And the control input $\boldsymbol{u}_s = [v_q, v_d]^T = \boldsymbol{u} + \boldsymbol{u}_{com} + \sigma_c$. According to the SDRE approach, the optimal control law is given by

$$\boldsymbol{u} = \boldsymbol{K}(\boldsymbol{x})\boldsymbol{x} - \boldsymbol{u_{com}} - \boldsymbol{\sigma_c} \tag{13}$$

where $\boldsymbol{K}(\boldsymbol{x}) = -\boldsymbol{T}^{-1}\boldsymbol{B}^T\Pi(\boldsymbol{x})$ is the gain matrix of the controller, and $\Pi(\boldsymbol{x}) \in \boldsymbol{R}^{3\times 3}$ is the positive-definite solution of the following state-dependent Riccati equation (SDRE) [38]:

$$\Pi(\boldsymbol{x})\boldsymbol{A}(\boldsymbol{x}) + \boldsymbol{A}^{\boldsymbol{T}}(\boldsymbol{x})\Pi(\boldsymbol{x}) - \Pi(\boldsymbol{x})\boldsymbol{B}\boldsymbol{T}^{-\boldsymbol{1}}\boldsymbol{B}^{\boldsymbol{T}}\Pi(\boldsymbol{x}) + \boldsymbol{Q} = 0 \tag{14}$$

where $\boldsymbol{Q} \in \boldsymbol{R}^{3\times 3}$ is a constant symmetric positive semi-definite weighting matrix and $\boldsymbol{T} \in \boldsymbol{R}^{2\times 2}$ is a constant symmetric positive definite weighting matrix. By employing the estimated $\boldsymbol{\sigma} = [\sigma_\omega, \sigma_q, \sigma_d]^T$ obtained by the proposed HODO, the i_{qd} and i_{dd} are estimated as

$$\hat{i}_{qd} = \frac{k_2\omega_d - k_{10} i_{dd} i_q - \hat{\sigma}_\omega}{k_1}$$
$$\hat{i}_{dd} = \frac{L_d - L_q}{\lambda_m}\hat{i}_{qd}^2. \tag{15}$$

By utilizing the disturbance $\boldsymbol{\sigma}$ estimated by the proposed HODO, the optimal control law becomes

$$\boldsymbol{u} = \boldsymbol{K}(\bar{\boldsymbol{x}})\bar{\boldsymbol{x}} - \hat{\boldsymbol{u}}_{\boldsymbol{com}} - \hat{\boldsymbol{\sigma}}_{\boldsymbol{c}} \tag{16}$$

where $\hat{\tilde{i}}_q = i_q - \hat{i}_{qd}$, $\hat{\tilde{i}}_d = i_d - \hat{i}_{dd}$, $\bar{\boldsymbol{x}} = [\tilde{\omega}\ \hat{\tilde{i}}_q\ \hat{\tilde{i}}_d]^T$, $\hat{\boldsymbol{\sigma}}_{\boldsymbol{c}} = [\hat{\sigma}_q\ \hat{\sigma}_d]^T$, and $\hat{\boldsymbol{u}}_{com}$ is obtained as

$$\hat{\boldsymbol{u}}_{\boldsymbol{com}} = \begin{bmatrix} \hat{u}_{cq} \\ \hat{u}_{cd} \end{bmatrix} = \begin{bmatrix} \frac{1}{k_5}\left(k_3\hat{i}_{qd} + k_4\omega_d + k_9\hat{\tilde{i}}_d\omega_d + k_9\hat{i}_{dd}\omega_r\right) \\ \frac{1}{k_7}\left(k_6\hat{i}_{dd} - k_8\hat{\tilde{i}}_q\omega_d - k_8\hat{i}_{qd}\omega_r\right) \end{bmatrix}.$$

Fig. 2 presents the overall control flowchart of the proposed HODO-based SDRE speed controller for an IPMSM drive. As shown in Fig. 2, the kth-order of the HODO is first determined based on *Remark 1* and then correspondingly the HODO gains $\boldsymbol{L} = [\boldsymbol{L}_0, \boldsymbol{L}_1, \ldots, \boldsymbol{L}_k]$ are selected by satisfying (5). It is noted that the order of the proposed HODO is fixed during the online testing which is selected in Section IV.B for the IPMSM drives based on the faster convergence rate, accurate disturbance estimation (i.e., smaller steady-state error), and reduced computational burden. Next, the estimated $\boldsymbol{\sigma}$ is provided to the SDRE-based speed controller to mitigate the disturbances, which results in the robust speed control of an IPMSM drive.

The $\bar{\boldsymbol{x}}$ in (16) can be written as

$$\bar{\boldsymbol{x}} = \boldsymbol{x} + \boldsymbol{H}_{12}\, e_\omega$$
$$\hat{\boldsymbol{\sigma}}_{\boldsymbol{c}} = \boldsymbol{\sigma_c} - \begin{bmatrix} e_q \\ e_d \end{bmatrix}$$
$$\hat{\boldsymbol{u}}_{\boldsymbol{com}} = \boldsymbol{H}_{34}\, e_\omega + \boldsymbol{u_{com}} \tag{17}$$

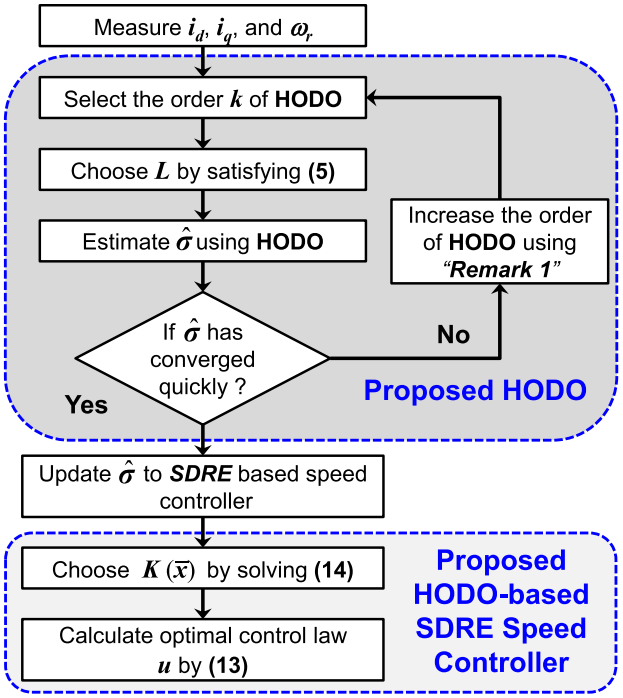

FIGURE 2. Overall control flowchart of the proposed HODO-based SDRE speed controller for an IPMSM drive.

where $\boldsymbol{x} = \left[\tilde{\omega}\ \tilde{i}_q\ \tilde{i}_d\right]^T$, $\boldsymbol{H}_{12} = [0\ h_1\ h_2]^T$, $h_1 = 1/k_1$, $h_2 = \frac{L_d - L_q}{k_1 \lambda_m}(i_{qd} + \hat{i}_{qd})$, $\boldsymbol{H}_{34} = [0\ h_3\ h_4]^T$, $e_\omega = \sigma_\omega - \hat{\sigma}_\omega$, $e_q = \sigma_q - \hat{\sigma}_q$, $e_d = \sigma_d - \hat{\sigma}_d$, $h_3 = \frac{1}{k_5}(k_3 h_1 + k_9 h_2 \omega_d + k_9 h_2 \omega_r)$, and $h_4 = \frac{1}{k_7}(k_6 h_2 - k_8 h_1 \omega_d - k_8 h_1 \omega_r)$.

Then, the control law (16) is rewritten to analyze the stability as

$$\boldsymbol{u} = -\boldsymbol{\sigma_c} + \boldsymbol{K}(\boldsymbol{x} + \boldsymbol{H}_{12} e_\omega)(\boldsymbol{x} + \boldsymbol{H}_{12} e_\omega) + \boldsymbol{M}\boldsymbol{e} - \boldsymbol{u_{com}} \quad (18)$$

where $\boldsymbol{M} = [\boldsymbol{K}(\boldsymbol{x} + \boldsymbol{H}_{12})(\boldsymbol{H}_{12} + \boldsymbol{H}_{34}) - \boldsymbol{I}_2]$ and $\boldsymbol{e} = [e_\omega\ e_q\ e_d]^T = [\sigma_\omega - \hat{\sigma}_\omega;\ \sigma_q - \hat{\sigma}_q;\ \sigma_d - \hat{\sigma}_d]^T$.

By substituting (18) into (11), the dynamic equation of the tracking error is given as

$$\begin{aligned} \dot{\boldsymbol{x}} &= (\boldsymbol{A} + \boldsymbol{B}\boldsymbol{K})\boldsymbol{x} + \boldsymbol{f}(\boldsymbol{x}, \boldsymbol{e}). \\ \dot{\boldsymbol{e}} &= \boldsymbol{L}\boldsymbol{e} \end{aligned} \quad (19)$$

where $\boldsymbol{f}(\boldsymbol{x},\boldsymbol{e})$ is the function of $\boldsymbol{x}$ and $\boldsymbol{e}$ such that $\boldsymbol{f}(\boldsymbol{x},\boldsymbol{e}) = \boldsymbol{f}_1(\boldsymbol{x},\boldsymbol{e})\ \boldsymbol{x} + \boldsymbol{f}_2(\boldsymbol{x},\boldsymbol{e})\ \boldsymbol{e}$. The augmented form of the (19) can be written as

$$\begin{bmatrix} \dot{\boldsymbol{x}} \\ \dot{\boldsymbol{e}} \end{bmatrix} = \begin{bmatrix} \boldsymbol{A} + \boldsymbol{B}\boldsymbol{K} & 0 \\ 0 & \boldsymbol{L} \end{bmatrix} \begin{bmatrix} \boldsymbol{x} \\ \boldsymbol{e} \end{bmatrix} + \begin{bmatrix} \boldsymbol{f}_1(\boldsymbol{x}, \boldsymbol{e}) & \boldsymbol{f}_2(\boldsymbol{x}, \boldsymbol{e}) \\ 0 & 0 \end{bmatrix} \begin{bmatrix} \boldsymbol{x} \\ \boldsymbol{e} \end{bmatrix}. \quad (20)$$

The above dynamic equation (20) along with the proposed HODO (4) and (5) forms the closed-loop system of the observer-based control system. By following the *Theorem 5.1* in [38], the tracking error $\boldsymbol{x}$ and estimation error $\boldsymbol{e}$ in (20) are asymptotically stable at zero by employing the observer-based control law (16) and the proposed HODO (4) such that the observer gains satisfy (5) [39].

TABLE 1. Specifications and nominal parameters of a prototype three-phase IPMSM drive used in the experimental testbed.

Quantity	Symbol	Value
Stator resistance	R_{s0}	2.48 Ω
q-axis inductance	L_{q0}	113.91 mH
d-axis inductance	L_{d0}	74.98 mH
Number of poles	p	4
Magnet flux linkage	λ_{m0}	0.193 Wb
Equivalent rotor inertia	J_0	0.00042 kg·m^2
Viscous friction coefficient	B_0	0.0001 N·m·s
dc-link voltage	V_{dc}	295 V
Sampling period	T_s	200 μs
Rated power	P_{rated}	390 W
Rated speed	ω_{rated}	523.3 rad/s
Rated load torque	$T_{L-rated}$	1.5 N·m
PWM switching frequency	f_s	5 kHz
Rated phase current	I_{rated}	1.3 A

Remark 4: The proposed HODO-based SDRE speed controller is updated by the $\hat{\sigma}_\omega$, $\hat{\sigma}_q$, and $\hat{\sigma}_d$ which can accurately estimate the parameter uncertainties and external load torque, so it has the superior speed tracking performance compared to the conventional SDRE speed controller [7] because the latter [7] has only the load torque observer that completely ignores the effects of the mechanical and electrical parameter uncertainties. Note that the [7] did not present the speed response under the mechanical parameter uncertainties that can seriously degrade the speed tracking performance of the conventional SDRE speed controller [7] because its SDRE observer cannot compensate for them. On the other hand, the proposed HODO-based SDRE speed controller can effectively estimate and compensate for the mechanical and electrical parameter uncertainties and external load torque disturbances of the IPMSM drives.

IV. VALIDATION AND IMPLEMENTATION UNDER DIFFERENT OPERATING SCENARIOS

This section presents the details of the experimental testbed used to validate the proposed HODO-based SDRE speed controller for an IPMSM drive. First, the optimum order k for the proposed HODO is selected to reduce the computational burden. Next, its accurate convergence is verified under a sudden step change of the crude values. Last, the comparative performance analysis between the proposed HODO, the conventional 1st-order DO [20] with a strict assumption (i.e., $\dot{\boldsymbol{\sigma}}(t) \approx 0$), the conventional GPIO [27], and the conventional SDRE observer [7] is presented with the SDRE-based speed controller [7].

A. DESCRIPTION OF EXPERIMENTAL TESTBED

Fig. 3 presents the overall experimental setup to demonstrate the effectiveness of the proposed HODO-based SDRE speed controller for an IPMSM drive. Table 1 presents the specifications and nominal parameters of a prototype three-phase IPMSM drive used in the experimental testbed. The control inputs $\boldsymbol{u}_d$ and $\boldsymbol{u}_q$ from the SDRE speed controller using the disturbances ($\hat{\sigma}_\omega$, $\hat{\sigma}_q$, and $\hat{\sigma}_d$) estimated by the proposed

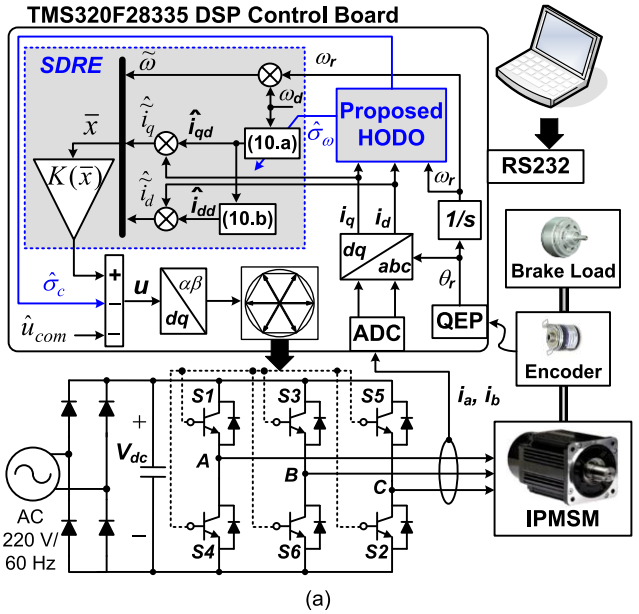

FIGURE 3. Overall experimental setup to execute the proposed HODO-based SDRE speed controller for an IPMSM drive. (a) Complete control schematic block diagram. (b) Experimental testbed.

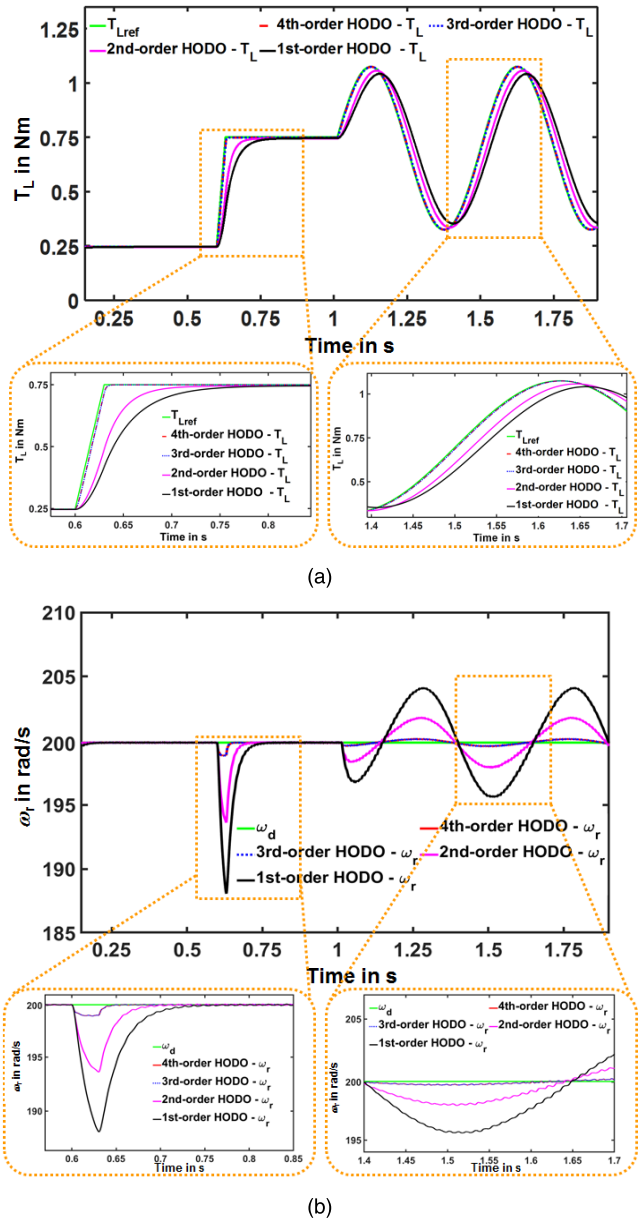

FIGURE 4. Comparative simulation results of T_L change for selecting the optimum order k of the proposed HODO with four different observer orders. (a) Estimated T_L. (b) Speed response ω_r.

HODO are implemented by the space vector pulse-width modulation (SVPWM) technique. In this paper, the number of the Taylor series members is selected as $N = 2$ to minimize the computational burden and assure the good tracking performance. The large tracking errors and control input values can be penalized by the weighting matrices chosen as $\boldsymbol{Q} = \text{diag}(1, 5, 5)$ and $\boldsymbol{T} = 10^{-3} \times \boldsymbol{I}_2$, which are tuned via Bryson's rule [32].

B. OPTIMUM ORDER CALCULATION FOR HODO

The optimum order k of the proposed HODO is calculated such that the fast convergence rate and accurate estimation of $\boldsymbol{\sigma}$ are achieved and the computational burden of the proposed HODO is significantly reduced. The main criteria to choose the optimum order k is the fast convergence rate, accurate convergence (i.e., smaller steady state error), and low computational burden. Thus the order k of the proposed HODO should be chosen so that the disturbance $\boldsymbol{\sigma}$ is supposed to have a bounded kth derivative as mentioned in *Remark 1*.

In this paper, Fig. 4(a) and (b) presents the tracking performance of the reference load torque T_{Lref} with a sudden step response at 0.6 s and a sinusoidal response at 1 s to investigate the comparative performance analysis of the proposed HODO with four different observer orders (i.e., the 1st-order, the 2nd-order, the 3rd-order, and the 4th-order HODOs), and simulations are carried out via a MATLAB/Simulink package. It can be deduced from (2) that the $\sigma_\omega = -k_{11}T_L$, in case of ignoring the parameter uncertainties and unmodeled dynamics, which implies that the estimated $T_L = -\sigma_\omega/k_{11}$. It is noted that the proposed HODO becomes the 1st-order DO if $\boldsymbol{L}_2 = \ldots = \boldsymbol{L}_k = 0$, the 2nd-order DO if $\boldsymbol{L}_3 = \ldots = \boldsymbol{L}_k = 0$, and the 3rd-order DO if $\boldsymbol{L}_4 = \ldots = \boldsymbol{L}_k = 0$. In this paper, the observer gains are chosen by satisfying (5) as the gains of the proposed HODO presented in Table 2 such that $k = 3$ to achieve a fast convergence rate.

As presented in Fig. 4(a), the convergence rates for the sudden step change of the 1st-order HODO, 2nd-order HODO, 3rd-order HODO, and 4th-order HODO are 0.2 s,

TABLE 2. Gains of the proposed HODO.

Quantity	Value
L_0	diag {560.42, 810.23, 835.75}
L_1	diag {320, 440, 445}
L_2	diag {770, 909.07, 945.5}
L_3	diag {890, 1030, 1050}

0.14 s, 0.03 s, and 0.03 s, respectively. In addition, during the sinusoidal load change, Fig. 4(a) presents that the time delay and steady-state error for the 1st-order HODO (0.045s, 0.033 N·m) and 2nd-order HODO (0.02s, 0.018 N·m) are larger than the 3rd-order HODO and 4th-order HODO (0.0001 s, 0.0001 N·m). In Fig. 4(a), the 1st-order HODO similar to [20] encounters the estimation error of the load torque disturbance with a non-zero derivative and the 2nd-order HODO shows the estimation error of the load torque disturbance in the scenario of the sinusoidal load torque change. Fig. 4(b) presents that the speed errors ω_e ($\omega_e = \omega_d - \omega_r$) of the 1st-order HODO and 2nd-order HODO are 12.5 rad/s and 6.1 rad/s during a sudden load change at 0.6s and 5 rad/s and 3 rad/s during a sinusoidal load change, respectively.

Next, as shown in Fig. 4(a), the 3rd-order HODO and the 4th-order HODO accurately estimate the load torque disturbances in both scenarios of a sudden step change and a sinusoidal change, which satisfy *Remark 1*. Meanwhile, as shown in Fig. 4(b), the 3rd-order HODO and 4th-order HODO has almost the same speed error, i.e., $\omega_e = 1.4$ rad/s for the sudden load step change and 0.15 rad/s for the sinusoidal load change. Therefore, the 3rd-order HODO and 4th-order HODO have the faster convergence rate and smaller steady-state error compared to the 1st-order HODO and 2nd-order HODO. Meanwhile, the computational burden of the 4th-order HODO is higher than that of the 3rd-order HODO. Therefore, in this paper, $k = 3$ is selected as the optimum order of the proposed HODO for the IPMSM drives based on the faster convergence rate, accurate disturbance estimation (i.e., smaller steady-state error), and reduced computational burden.

C. ACCURATE CONVERGENCE EVALUATION OF THE HODO UNDER THE CRUDE VALUES OF THE IPMSM PARAMETERS

The performance of the proposed HODO is examined under worst possible set of the crude values for the IPMSM mechanical and electrical parameters to prove the accurate convergence of the lumped disturbances (σ_ω, σ_q, and σ_d) at the ω_d of 300 rad/s and the T_L of 1 N·m in the controller. First, Fig. 5(a) presents the estimated values of the σ_ω, σ_q, and σ_d with the crude values of the IPMSM mechanical parameters set as $J = 80\%\ J_0$ and $B = 120\%\ B_0$. As shown in Fig. 5(a), the proposed HODO quickly estimates the σ_ω (−4895 V to −5200 V), σ_q (11.2 V), and σ_d (−13.1 V) with a settling time (t_s) of 15 ms when the mechanical uncertainties are suddenly applied. As the σ_ω defined in (2) contains $-k_{11}T_L$ along with the parameter variations, so the value of the estimated σ_ω is in the range of kV.

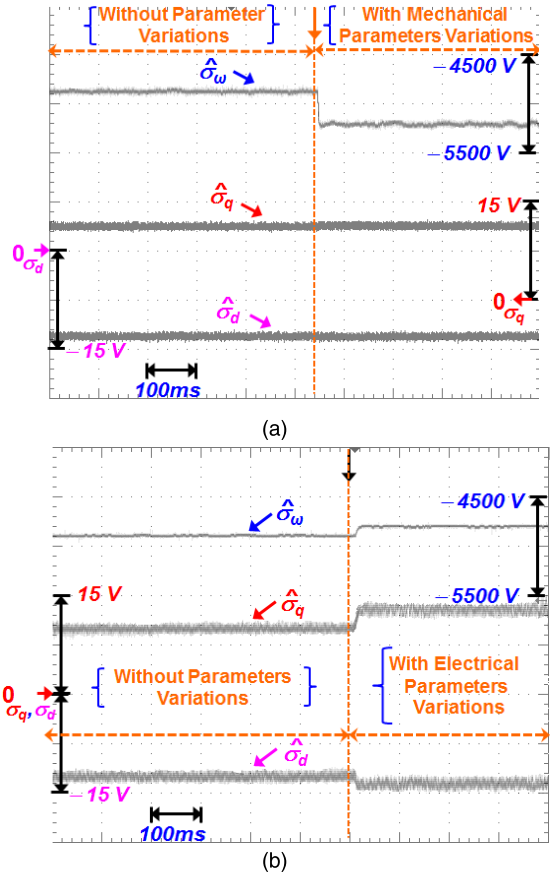

FIGURE 5. Experimental results of the proposed HODO-based SDRE speed controller under crude initial values. (a) $\hat{\sigma}_\omega$, $\hat{\sigma}_q$, and $\hat{\sigma}_d$ under $J = 80\%\ J_0$ and $B = 120\%\ B_0$. (b) $\hat{\sigma}_\omega$, $\hat{\sigma}_q$, and $\hat{\sigma}_d$ under $L_d = 80\%\ L_{d0}$, $L_q = 70\%\ L_{q0}$, $\lambda_m = 80\%\lambda_{m0}$, and $R_s = 150\%\ R_{s0}$.

Next, Fig. 5(b) shows the estimated values of the σ_ω, σ_q, and σ_d with the crude values of the IPMSM electrical parameters set as $L_d = 80\%\ L_{d0}$, $L_q = 70\%\ L_{q0}$, $\lambda_m = 80\%\ \lambda_{m0}$, and $R_s = 150\%\ R_{s0}$. When the electrical parameter uncertainties are suddenly applied as shown in Fig. 5(b), the proposed HODO quickly estimates the changes in the disturbances with a settling time (t_s) of 18 ms, (i.e., $\hat{\sigma}_\omega(-4897\ \text{V} \rightarrow -4800\ \text{V})$, $\hat{\sigma}_q(11.2\ \text{V} \rightarrow 13.6\ \text{V})$, and $\hat{\sigma}_d\ (-13.1\ \text{V} \rightarrow -14.3\ \text{V})$). Fig. 5(a) and (b) show that the $\hat{\sigma}_\omega$, $\hat{\sigma}_q$, and $\hat{\sigma}_d$ converge to their actual values within $t_s = 20$ ms, which verifies that the proposed HODO quickly calculates the estimated lumped disturbances with a smaller t_s.

D. COMPARATIVE EXPERIMENTAL PERFORMANCE EVALUATION FOR ABRUPT LOAD CHANGE WITH PARAMETER UNCERTAINTIES

First, the comparative experimental results of the SDRE-based speed controller [7] with three different observers are presented under an abrupt load change, i.e., T_L is suddenly changed from 0.75 N·m to 1.5 N·m at constant ω_d of 300 rad/s. Practically, the unmodeled dynamics and parameter uncertainties are always present in the IPMSM drive, which can significantly deteriorate the transient and steady-state performance of the SDRE-based speed controller.

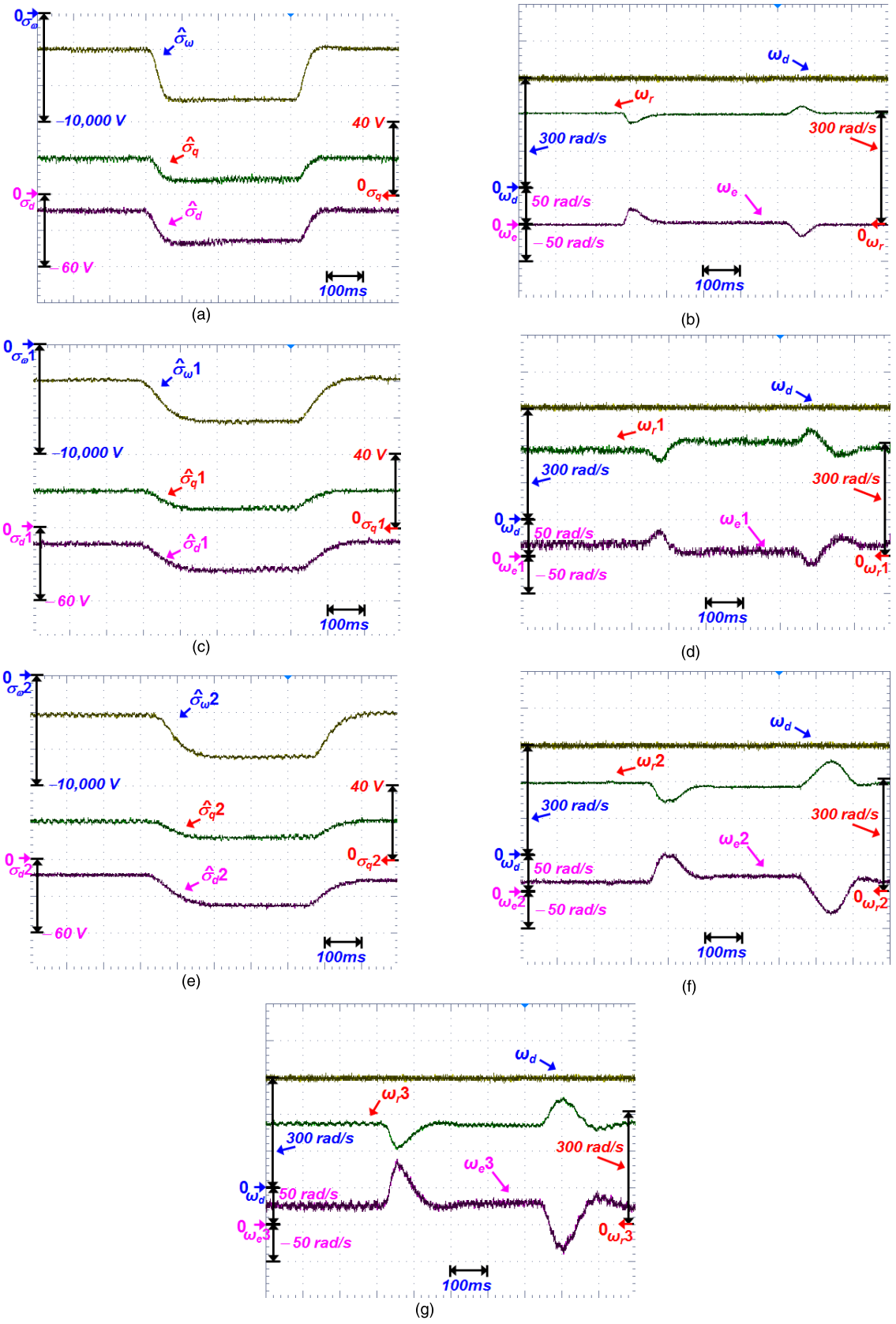

FIGURE 6. Experimental results of the SDRE-based speed controller under an abrupt load change. (a) Proposed HODO: $\hat{\sigma}_\omega$, $\hat{\sigma}_q$, and $\hat{\sigma}_d$. (b) Proposed HODO: ω_d, ω_r, and ω_e. (c) Conventional 1st-order DO [20]: $\hat{\sigma}_\omega 1$, $\hat{\sigma}_q 1$, and $\hat{\sigma}_d 1$. (d) Conventional 1st-order DO [20]: ω_d, $\omega_r 1$, and $\omega_e 1$. (e) Conventional GPIO [27]: $\hat{\sigma}_\omega 2$, $\hat{\sigma}_q 2$, and $\hat{\sigma}_d 2$. (f) Conventional GPIO [27]: ω_d, $\omega_r 2$, and $\omega_e 2$. (g) Conventional SDRE observer [7]: ω_d, $\omega_r 3$, and $\omega_e 3$.

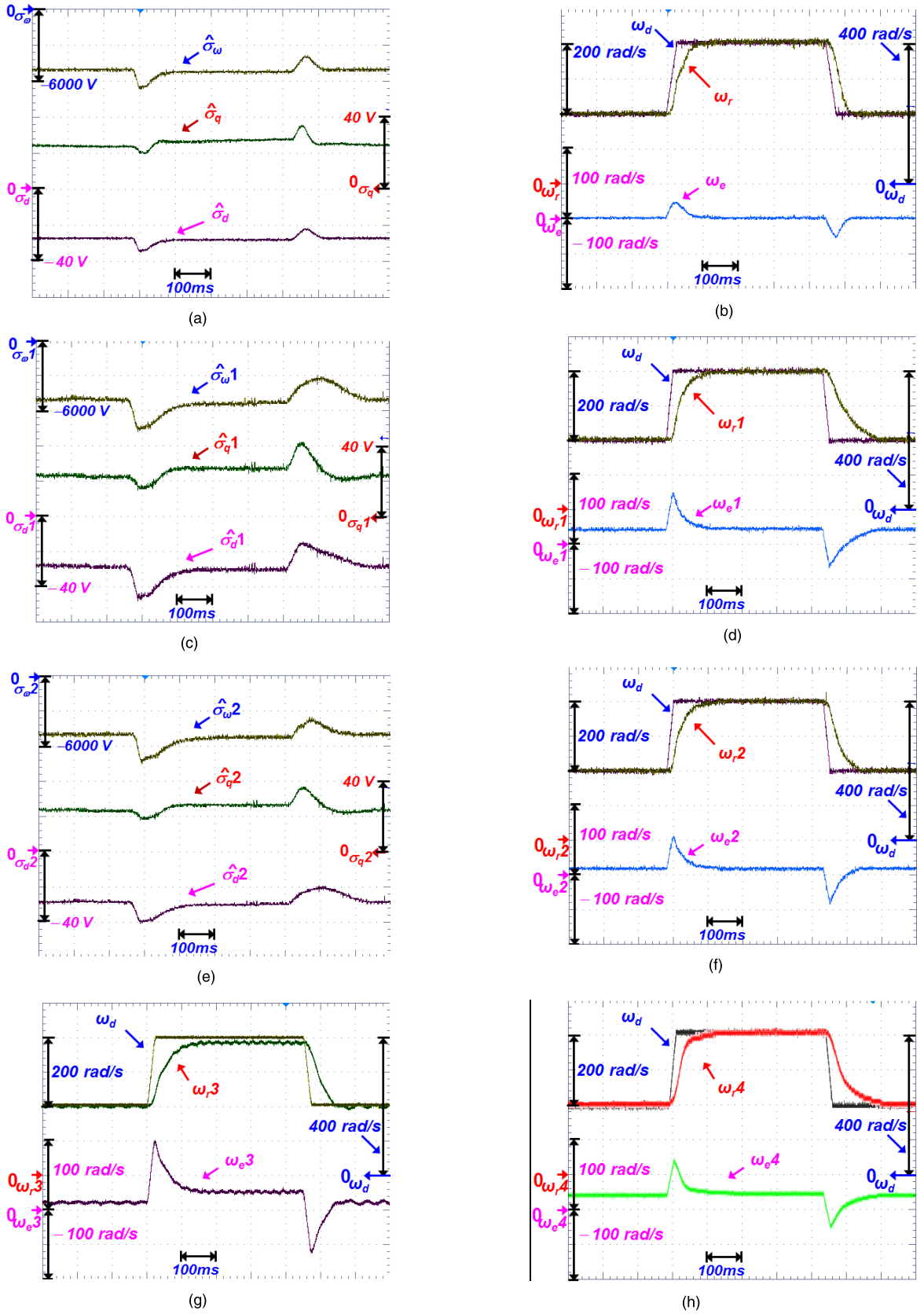

FIGURE 7. Experimental results of the SDRE-based speed controller under an abrupt speed change. (a) Proposed HODO: $\hat{\sigma}_\omega$, $\hat{\sigma}_q$, and $\hat{\sigma}_d$. (b) Proposed HODO: ω_d, ω_r, and ω_e. (c) Conventional 1st-order DO [20]: $\hat{\sigma}_\omega 1$, $\hat{\sigma}_q 1$, and $\hat{\sigma}_d 1$. (d) Conventional 1st-order DO [20]: ω_d, $\omega_r 1$, and $\omega_e 1$. (e) Conventional GPIO [27]: $\hat{\sigma}_\omega 2$, $\hat{\sigma}_q 2$, and $\hat{\sigma}_d 2$. (f) Conventional GPIO [27]: ω_d, $\omega_r 2$, and $\omega_e 2$. (g) Conventional SDRE observer [7]: ω_d, $\omega_r 3$, and $\omega_e 3$. (h) Conventional EKF [18]: ω_d, $\omega_r 4$, and $\omega_e 4$.

However, the parameter uncertainties (i.e., mechanical parameters (i.e., 150% B_0, 150% J_0) and electrical parameters (i.e., 80%L_{d0}, 80% L_{q0}, 150% R_{s0}, and 90% λ_{m0})) are added to emphasize the superiority of the proposed HODO compared to the conventional 1st-order DO, the conventional GPIO, and the conventional SDRE observer. Fig. 6(a) presents that the $\hat{\sigma}_\omega$ (-3346 V $\rightarrow$ -8653 V), $\hat{\sigma}_q$ (20.4 V $\rightarrow$ 10.6 V), and $\hat{\sigma}_d$ (-12.6 V $\rightarrow$ -40.8 V) estimated by the proposed HODO converge with t_s of 78 ms, 75 ms, and 76 ms, respectively. Fig. 6(c)$-$(f) present the experimental waveforms of the SDRE-based speed controller with the conventional 1st-order DO (i.e., $\hat{\sigma}_\omega 1$ (t_s = 198 ms), $\hat{\sigma}_q 1$ (t_s = 179 ms), $\hat{\sigma}_d 1$ (t_s = 185 ms), $\omega_r 1$ (t_s = 164 ms)) and the conventional GPIO (i.e., $\hat{\sigma}_\omega 2$ (t_s = 190 ms), $\hat{\sigma}_q 2$ (t_s = 171 ms), $\hat{\sigma}_d 2$ (t_s = 175 ms), $\omega_r 2$ (t_s = 145 ms)) under a sudden load change. Fig. 6(a), (c), and (e) highlight that the proposed HODO (t_s = 78 ms) has a faster convergence rate compared to the conventional 1st-order DO (t_s = 198 ms) and the conventional GPIO (t_s = 190 ms). The comparative results of Fig. 6(b), (d), (f), and (g) demonstrate that the speed error ω_e of the proposed HODO (ω_e = 23 rad/s) has been significantly reduced compared with those of the conventional 1st-order DO ($\omega_e 1 = 41$ rad/s), the conventional GPIO ($\omega_e 2 = 48$ rad/s), and the conventional SDRE observer ($\omega_e 3 = 89$ rad/s).

E. COMPARATIVE EXPERIMENTAL PERFORMANCE EVALUATION FOR ABRUPT SPEED CHANGE WITH PARAMETER UNCERTAINTIES

Next, the comparative experimental results of the SDRE-based speed controller [7] with three different observers are presented under an abrupt speed change, i.e., ω_d is suddenly changed from 200 rad/s to 400 rad/s at the T_L of 1 N·m. Note that the parameter uncertainties in the mechanical parameters (i.e., 150% B_0, 150% J_0,) and electrical parameters (i.e., 80%L_{d0}, 80% L_{q0}, 150% R_{s0}, and 90% λ_{m0}) are considered to verify the robustness of the proposed HODO-based SDRE speed controller.

Note that the parameter uncertainties in the mechanical parameters (i.e., 150% B_0, 150% J_0,) and electrical parameters (i.e., 80% L_{d0}, 80% L_{q0}, 150% R_{s0}, and 90% λ_{m0}) are considered to verify the robustness of the proposed HODO-based SDRE speed controller. Fig. 7(a) shows the $\hat{\sigma}_\omega$, $\hat{\sigma}_q$, and $\hat{\sigma}_d$ estimated by the proposed HODO within t_s = 80 ms, whereas the conventional 1st-order DO (t_s = 165 ms) in Fig. 7(c) and the conventional GPIO (t_s = 145 ms) in Fig. 7(e) have a very slow convergence rate which also leads to the slow response of ω_r. By utilizing the $\hat{\sigma}_\omega$ (-4861 V $\rightarrow$ -5280 V), $\hat{\sigma}_q$ (24.4 V $\rightarrow$ 27.6 V), and $\hat{\sigma}_d$ (-27.2 V $\rightarrow$ -28.4 V) estimated by the proposed HODO, it is observed in Fig. 7(b), (d), and (f) that the transient and steady-state speed errors ω_e of the SDRE-based speed controller with the proposed HODO (26 rad/s and 4.2 rad/s) are significantly reduced compared to those of the conventional 1st-order DO (71 rad/s and 19 rad/s) and the conventional GPIO (53 rad/s and 10.5 rad/s). Fig. 7(g) shows the experimental results of the conventional SDRE observer [7] indicating the higher transient and steady-state speed errors ω_e of 97 rad/s and 29 rad/s, respectively. Fig. 7(h) presents the experimental results of the conventional EKF [18] such that the speed errors ω_e during the transient and steady-state are 68 rad/s and 20 rad/s, respectively. Hence, the transient and steady-state performance is significantly improved by quickly estimating the disturbances with the proposed HODO. Table 3 summarizes the comparative performance of the SDRE-based speed controller [7] with the proposed HODO, the conventional 1st-order DO [20], the conventional GPIO [27], the conventional SDRE observer [7], and the conventional EKF [18].

TABLE 3. Summary of the comparative performance analysis of the proposed NOC and conventional NOC.

Criteria	Abrupt Load Change (①/②/③)	Abrupt Speed Change (①/②/③)
$\hat{\sigma}_\omega$ (V)	–8653 / –7233 / –7466	–5280 / –5340 / –5307
$\hat{\sigma}_q$ (V)	10.6 / 11.4 / 10.9	27.6 / 28.4 / 27.1
$\hat{\sigma}_d$ (V)	–40.8 / –36.4 / –38.1	–28.4 / –31.2 / –26.8
Criteria	Abrupt Load Change (①/②/③/④)	Abrupt Speed Change (①/②/③/④/⑤)
ω_e (rad/s)	23 / 41 / 48 / 89	26 / 71 / 53 / 97 / 68
t_s (ms)	80 / 164 / 145 / 210	88 / 140 / 130 / 172 / 121

Note that the "①", "②", "③", "④", and "⑤" represent the SDRE-based speed controller [7] with the proposed HODO, the conventional 1st-order DO [20], the conventional GPIO [27], the conventional SDRE observer [7], and the conventional EKF [18], respectively.

V. CONCLUSION

This paper presents a robust high-order disturbance observer (HODO) design for the SDRE-based speed controller of an IPMSM drive. The lumped disturbances (i.e., external load torque, parameter uncertainties, etc.) estimated by the proposed HODO are utilized to reject the disturbances encountered by an SDRE-based speed controller of an IPMSM drive. The practicality and efficacy of the proposed HODO are confirmed by comparing with the conventional 1st-order DO and conventional GPIO via the MATLAB/Simulink based simulation results and IPMSM test-bed based experimental results with TI TMS320F28335 DSP. Moreover, by keeping the excellent performance of the HODO for the disturbance estimation and compensation, the proposed HODO can be integrated with various advanced control techniques such as model predictive control, sliding mode control, fuzzy logic control, etc.

REFERENCES

[1] W. Zine, Z. Makni, E. Monmasson, L. Idkhajine, and B. Condamin, "Interests and limits of machine learning-based neural networks for rotor position estimation in EV traction drives," *IEEE Trans. Ind. Informat.*, vol. 14, no. 5, pp. 1942–1951, May 2018.

[2] D. Q. Dang, N. T.-T. Vu, H. H. Choi, and J.-W. Jung, "Neuro-fuzzy control of interior permanent magnet synchronous motors: Stability analysis and implementation," *J. Elect. Eng. Technol.*, vol. 8, no. 6, pp. 1439–1450, Nov. 2013.

[3] J. Yang, W.-H. Chen, S. Li, L. Guo, and Y. Yan, "Disturbance/uncertainty estimation and attenuation techniques in PMSM drives—A survey," *IEEE Trans. Ind. Electron.*, vol. 64, no. 4, pp. 3273–3285, Apr. 2017.
[4] Y. A.-R. I. Mohamed and E. F. El-Saadany, "A current control scheme with an adaptive internal model for torque ripple minimization and robust current regulation in PMSM drive systems," *IEEE Trans. Energy Convers.*, vol. 23, no. 1, pp. 92–100, Mar. 2008.
[5] K. Cho, J. Kim, S. B. Choi, and S. Oh, "A high-precision motion control based on a periodic adaptive disturbance observer in a PMLSM," *IEEE/ASME Trans. Mechatronics*, vol. 20, no. 5, pp. 2158–2171, Oct. 2015.
[6] Y. Zhang, C. M. Akujuobi, W. H. Ali, C. L. Tolliver, and L. S. Shieh, "Load disturbance resistance speed controller design for PMSM," *IEEE Trans. Ind. Electron.*, vol. 53, no. 4, pp. 1198–1208, Jun. 2006.
[7] T. D. Do, S. Kwak, H. H. Choi, and J.-W. Jung, "Suboptimal control scheme design for interior permanent-magnet synchronous motors: An SDRE-based approach," *IEEE Trans. Power Electron.*, vol. 29, no. 6, pp. 3020–3031, Jun. 2014.
[8] W. Chen, J. Yang, L. Guo, and S. Li, "Disturbance-observer-based control and related methods-an overview," *IEEE Trans. Ind. Electron.*, vol. 63, no. 2, pp. 1083–1095, Feb. 2016.
[9] X. Zhang, L. Sun, K. Zhao, and L. Sun, "Nonlinear speed control for PMSM system using sliding-mode control and disturbance compensation techniques," *IEEE Trans. Power Electron.*, vol. 28, no. 3, pp. 1358–1365, Mar. 2013.
[10] G. Zhu, L.-A. Dessaint, O. Akhrif, and A. Kaddouri, "Speed tracking control of a permanent-magnet synchronous motor with state and load torque observer," *IEEE Trans. Ind. Electron.*, vol. 47, no. 2, pp. 346–355, Apr. 2000.
[11] T. D. Do, H. H. Choi, and J. W. Jung, "SDRE-based near optimal control design for PM synchronous motor," *IEEE Trans. Ind. Electron.*, vol. 59, no. 11, pp. 4063–4074, Nov. 2012.
[12] O. Wallscheid, E. F. B. Ngoumtsa, and J. Böcker, "Hierarchical model predictive speed and current control of an induction machine drive with moving-horizon load torque estimator," in *Proc. IEEE Int. Electr. Mach. Drives Conf. (IEMDC)*, San Diego, CA, USA, May 2019, pp. 2188–2195.
[13] A. Andersson and T. Thiringer, "Motion sensorless IPMSM control using linear moving horizon estimation with luenberger observer state feedback," *IEEE Trans. Transport. Electrific.*, vol. 4, no. 2, pp. 464–473, Jun. 2018.
[14] F.-J. Lin, Y.-C. Hung, J.-M. Chen, and C.-M. Yeh, "Sensorless IPMSM drive system using saliency back-EMF-based intelligent torque observer with MTPA control," *IEEE Trans. Ind. Informat.*, vol. 10, no. 2, pp. 1226–1241, May 2014.
[15] Y. Feng, X. Yu, and F. Han, "High-order terminal sliding-mode observer for parameter estimation of a permanent-magnet synchronous motor," *IEEE Trans. Ind. Electron.*, vol. 60, no. 10, pp. 4272–4280, Oct. 2013.
[16] X. Zhang and Z. Li, "Sliding-mode observer-based mechanical parameter estimation for permanent magnet synchronous motor," *IEEE Trans. Power Electron.*, vol. 31, no. 8, pp. 5732–5745, Aug. 2016.
[17] S. Hanke, S. Peitz, O. Wallscheid, J. Böcker, and M. Dellnitz, "Finite-control-set model predictive control for a permanent magnet synchronous motor application with online least squares system identification," in *Proc. IEEE Int. Symp. Predictive Control Elect. Drives Power Electron. (PRECEDE)*, Quanzhou, China, May/Jun. 2019, pp. 1–6.
[18] T. Boileau, N. Leboeuf, B. Nahid-Mobarakeh, and F. Meibody-Tabar, "Online identification of PMSM parameters: Parameter identifiability and estimator comparative study," *IEEE Trans. Ind. Appl.*, vol. 47, no. 4, pp. 1944–1957, Jul./Aug. 2011.
[19] M. Rashed, P. F. A. MacConnell, A. F. Stronach, and P. Acarnley, "Sensorless indirect-rotor-field-orientation speed control of a permanent-magnet synchronous motor with stator-resistance estimation," *IEEE Trans. Ind. Electron.*, vol. 54, no. 3, pp. 1664–1675, Jun. 2007.
[20] R. Errouissi, M. Ouhrouche, W.-H. Chen, and A. M. Trzynadlowski, "Robust cascaded nonlinear predictive control of a permanent magnet synchronous motor with antiwindup compensator," *IEEE Trans. Ind. Electron.*, vol. 59, no. 8, pp. 3078–3088, Aug. 2012.
[21] K.-H. Kim and M.-J. Youn, "A simple and robust digital current control technique of a PM synchronous motor using time delay control approach," *IEEE Trans. Power Electron.*, vol. 16, no. 1, pp. 72–82, Jan. 2001.
[22] W.-H. Chen, D. J. Ballance, P. J. Gawthrop, and J. O'Reilly, "A nonlinear disturbance observer for robotic manipulators," *IEEE Trans. Ind. Electron.*, vol. 47, no. 4, pp. 932–938, Aug. 2000.
[23] K.-H. Kim, I.-C. Baik, G.-W. Moon, and M.-J. Youn, "A current control for a permanent magnet synchronous motor with a simple disturbance estimation scheme," *IEEE Trans. Control Syst. Technol.*, vol. 7, no. 5, pp. 630–633, Sep. 1999.
[24] Y. X. Su, C. H. Zheng, and B. Y. Duan, "Automatic disturbances rejection controller for precise motion control of permanent-magnet synchronous motors," *IEEE Trans. Ind. Electron.*, vol. 52, no. 3, pp. 814–823, Jun. 2005.
[25] X. Zhang and G. H. B. Foo, "A constant switching frequency-based direct torque control method for interior permanent-magnet synchronous motor drives," *IEEE/ASME Trans. Mechatronics*, vol. 21, no. 3, pp. 1445–1456, Jun. 2016.
[26] D. Q. Dang, M. S. Rafaq, H. H. Choi, and J.-W. Jung, "Online parameter estimation technique for adaptive control applications of interior PM synchronous motor drives," *IEEE Trans. Ind. Electron.*, vol. 63, no. 3, pp. 1438–1449, Mar. 2016.
[27] H. Sira-Ramírez, J. Linares-Flores, C. García-Rodríguez, and M. A. Contreras-Ordaz, "On the control of the permanent magnet synchronous motor: An active disturbance rejection control approach," *IEEE Trans. Control Syst. Technol.*, vol. 22, no. 5, pp. 2056–2063, Sep. 2014.
[28] Y. Yan, J. Yang, Z. Sun, C. Zhang, S. Li, and H. Yu, "Robust speed regulation for PMSM servo system with multiple sources of disturbances via an augmented disturbance observer," *IEEE/ASME Trans. Mechatronics*, vol. 23, no. 2, pp. 769–780, Apr. 2018.
[29] K. Liu, J. Feng, S. Guo, L. Xiao, and Z.-Q. Zhu, "Identification of flux linkage map of permanent magnet synchronous machines under uncertain circuit resistance and inverter nonlinearity," *IEEE Trans. Ind. Informat.*, vol. 14, no. 2, pp. 556–568, Feb. 2018.
[30] Z. Yang, B. Meng, and H. Sun, "A new kind of nonlinear disturbance observer for nonlinear systems with applications to cruise control of air-breathing hypersonic vehicles," *Int. J. Control*, vol. 90, no. 9, pp. 1935–1950, Sep. 2016.
[31] C. Zhang, Y. Yan, C. Wen, J. Yang, and H. Yu, "A nonsmooth composite control design framework for nonlinear systems with mismatched disturbances: Algorithms and experimental tests," *IEEE Trans. Ind. Electron.*, vol. 65, no. 11, pp. 8828–8839, Nov. 2018.
[32] F. Lin, *Robust Control Design: An Optimal Control Approach*. Chichester, U.K.: Wiley, 2007.
[33] K. Ogata, *Modern Control Engineering*, 5th ed. Englewood Cliffs, NJ, USA: Prentice-Hall.
[34] T. Gao, Y.-J. Liu, L. Liu, and D. Li, "Adaptive neural network-based control for a class of nonlinear pure-feedback systems with time-varying full state constraints," *IEEE/CAA J. Automatica Sinica*, vol. 5, no. 5, pp. 923–933, Sep. 2018.
[35] L. Xiaoquan, L. Heyun, and H. Junlin, "Load disturbance observer-based control method for sensorless PMSM drive," *IET Electr. Power Appl.*, vol. 10, no. 8, pp. 735–743, Sep. 2016.
[36] D. Yoo, S. S.-T. Yau, and Z. Gao, "Optimal fast tracking observer bandwidth of the linear extended state observer," *Int. J. Control*, vol. 80, no. 1, pp. 102–111, Jan. 2007.
[37] Z. Gao, "Scaling and bandwidth-parameterization based controller tuning," in *Proc. Amer. Control Conf.*, Denver, CO, USA, vol. 6, 2003, pp. 4989–4996.
[38] H. T. Bank, B. M. Lewis, and H. T. Tran, "Nonlinear feedback controllers and compensators: A state-dependent Riccati equation approach," *J. Comput. Optim. Appl.*, vol. 37, no. 2, pp. 177–218, Mar. 2007.
[39] A. Isidori, *Nonlinear Control Systems*. London, U.K.: Springer-Verlag, 1995.

MUHAMMAD SAAD RAFAQ received the B.S. degree in electrical engineering from the University of Engineering and Technology, Taxila, Pakistan, in 2011, and the Ph.D. degree from the Division of Electronics and Electrical Engineering, Dongguk University, Seoul, South Korea, in 2019.

From 2012 to 2013, he was a Laboratory Engineer with the University of Gujrat, Gujrat, Pakistan. His research interests include distributed generation systems, control of power converters, parameter identification, electric vehicles, and DSP-based electric machine drives.

ANH TUAN NGUYEN received the B.S. and M.S. degrees in electrical engineering from the Hanoi University of Science and Technology, Hanoi, Vietnam, in 2010 and 2012, respectively, and the M.S. degree in electrical engineering from the Grenoble Institute of Technology, Joseph Fourier University, Grenoble, France, in 2015. He is currently pursuing the Ph.D. degree with the Division of Electronics and Electrical Engineering, Dongguk University, Seoul, South Korea.

His research interests include electric power systems, control of power converters, and DSP-based electric machine drives.

HAN HO CHOI (M'03) received the B.S. degree in control and instrumentation engineering from Seoul National University, Seoul, South Korea, in 1988, and the M.S. and Ph.D. degrees in electrical engineering from the Korea Advanced Institute of Science and Technology, Daejeon, South Korea, in 1990 and 1994, respectively.

He is currently with the Division of Electronics and Electrical Engineering, Dongguk University, Seoul. His research interests include control theory and its applications to real-world problems.

JIN-WOO JUNG (M'06) received the B.S. and M.S. degrees in electrical engineering from Hanyang University, Seoul, South Korea, in 1991 and 1997, respectively, and the Ph.D. degree in electrical and computer engineering from The Ohio State University, Columbus, OH, USA, in 2005.

From 1997 to 2000, he was with the Home Appliance Research Laboratory, LG Electronics Company Ltd., Seoul. From 2005 to 2008, he was a Senior Engineer with the Research and Development Center and with the PDP Development Team, Samsung SDI Company Ltd., South Korea. Since 2008, he has been a Professor with the Division of Electronics and Electrical Engineering, Dongguk University, Seoul. His research interests include DSP-based electric machine drives, distributed generation systems using renewable energy sources, and power conversion systems and drives for electric vehicles.